A parametric method for non-stationary interference suppression in direct sequence spread-spectrum systems

Slobodan Djukanović, Vesna Popović, Miloš Daković, LJubiša Stanković

Abstract— **The problem of non-stationary interference suppression in direct sequence spread-spectrum (DS-SS) systems is considered. The phase of interference is approximated by a polynomial within the considered interval. According to the local polynomial Fourier transform (LPFT) principle, the received signal is dechirped by using the obtained phase approximation and the interference is, in turn, suppressed by excising the corrupted low-pass frequency band. For the estimation of polynomial coefficients, we use the product high-order ambiguity function (PHAF), known for its capability to successfully resolve components of a multicomponent polynomial-phase signal (PPS). The proposed method can suppress interferences with both polynomial and non-polynomial phase. In addition, it can suppress both monocomponent and multicomponent interferences. The simulations show that the proposed method outperforms time-frequency (TF) methods, that successfully deal with multicomponent interferences, in terms of the error probability and computational complexity.**

I. Introduction

Direct sequence spread-spectrum (DS-SS) systems [1] are characterized by inherent interference rejection capability, which makes them suitable for use in congested communication channels. However, a strong interference (jammer) superimposed on the transmitted SS signal can severely deteriorate the performance of DS-SS receiver. To this end, numerous jammer suppression techniques have been proposed in order to enhance the DS-SS receiver's performance in severe jamming environments [2–7]. Time-frequency (TF) based methods [8] are effective in suppressing broadband interferences characterized by narrow instantaneous bandwidths. Methods based on linear TF representations can filter the corrupted SS signal in the transform domain; corresponding synthesis procedures output the jammer-free signal. Proposed linear TF methods include the short-time Fourier transform (STFT) [3], the fractional Fourier transform [4], and the local polynomial Fourier transform (LPFT) [5, 6]. In these papers, the jammer removal is accomplished via a binary mask, applied in the transform domain, which excises the corrupted frequency bins of the representation.

The Weierstrass's theorem [9] states that an arbitrary time-varying phase can be well approximated by a polynomial within the observed finite interval. Many methods for the estimation of phase coefficients of a polynomial-phase signal (PPS) have been proposed in the literature [10–15]. One of the most popular is the high-order ambiguity function (HAF), originally referred to as the polynomial-phase transform (PPT) [12]. The HAF, however, suffers from the identifiability problem when components of a multicomponent PPS have the same highest order phase coefficients, a situation encountered in multipath channels and SAR systems [16]. In order to overcome this problem, Barbarossa *et al.* proposed the product high-order ambiguity function (PHAF) [14].

We propose a method for the jammer suppression that uses the LPFT principle and the PHAF as the means of phase estimation. After the phase is estimated by a polynomial, the corrupted received signal is dechirped. In the Fourier transform of the dechirped signal, the jammer will be concentrated in the low-pass band, and therefore it can be suppressed by excising corrupted low-pass frequencies. The phase estimation, jammer excision and reconstruction of a jammer-free received signal are

Signal Processing, Vol. 91, No. 6, June 2011.

the steps of the proposed jammer suppression algorithm. The algorithm also deals with jammers with non-polynomial phase, which is achieved by narrowing the observed time interval. Moreover, owing to the ability of the PHAF to unambiguously estimate components of multicomponent signals, the algorithm can be easily extended to suppress multicomponent jammers.

Paper is organized as follows. Section 2 covers the theoretical background regarding the LPFT, PHAF and DS-SS systems. The proposed method is introduced in Section 3, where algorithms for both monocomponent and multicomponent jammers suppression are presented. Simulations are presented in Section 4, and conclusions are drawn in Section 5.

II. Theoretical background

A. Local polynomial Fourier transform

The Mth order discrete form of the LPFT of a signal $x(n)$ is defined by [6,17]

$$\begin{aligned}\mathrm{LPFT}\,(n,k) &= \sum_{m} x\,(n+m)\,w\,(m) \\ &\times e^{-j\sum\limits_{i=1}^{M}\omega_i\frac{m^{i+1}}{(i+1)!}} e^{-j\frac{2\pi}{N}mk} \\ &= \mathrm{DFT}_k\left[x\,(n+m)\,w\,(m)\,e^{-j\sum\limits_{i=1}^{M}\omega_i\frac{m^{i+1}}{(i+1)!}}\right]\end{aligned} \tag{1}$$

where $w\,(m)$ represents the analysis window of length N, ω_i is the ith transform parameter and $\mathrm{DFT}_k\,[\cdot]$ represents the discrete Fourier transform operator. If $x(n)$ is a monocomponent PPS, the LPFT can represent the ideal TF representation of $x(n)$ for an appropriate choice of the order M and parameters ω_i, $i = 1, 2, \cdots, M$. In reality, however, parameter estimation is performed over a multidimensional space, implying high computational complexity [5]. The parameters of PPSs can be estimated using different, computationally less demanding approach, described in the following section.

B. Product high-order ambiguity function

The most common model used in parametric analysis of non-stationary signals is a PPS model. The HAF was proposed to deal with PPSs, both monocomponent and multicomponent [12,13]; however, it suffers from the identifiability problem when components of a multicomponent PPS have the same highest order phase coefficients. This problem can be resolved by using the PHAF [14].

First, we define the multilag high-order instantaneous moment (ml-HIM) of a signal $x\,(n)\,, n = 0, \cdots, N-1$, in the following manner:

$$\begin{aligned} x_1(n) &= x(n) \\ x_2(n;\boldsymbol{\tau}_1) &= x_1(n+\tau_1)x_1^*(n-\tau_1), \\ x_3(n;\boldsymbol{\tau}_2) &= x_2(n+\tau_2;\boldsymbol{\tau}_1)x_2^*(n-\tau_2;\boldsymbol{\tau}_1), \\ &\vdots \\ x_P(n;\boldsymbol{\tau}_{P-1}) &= x_{P-1}(n+\tau_{P-1};\boldsymbol{\tau}_{P-2}) \\ &\times x_{P-1}^*(n-\tau_{P-1};\boldsymbol{\tau}_{P-2}), \end{aligned} \tag{2}$$

where $\boldsymbol{\tau}_i = [\tau_1, \tau_2, \cdots, \tau_i]$, $i = 1, ..., P-1$, are sets of used time lags. In $x_k\,(n;\boldsymbol{\tau}_{k-1})$, $k = 1, 2, \cdots, P$, index n goes from $\sum_{i=1}^{k-1}\tau_i$ to $N - \sum_{i=1}^{k-1}\tau_i - 1$. The multilag HAF (ml-HAF) is defined as the DFT of the ml-HIM,

$$X_P(f;\boldsymbol{\tau}_{P-1}) = \sum_{n=0}^{N-2\sum_{k=0}^{P-1}\tau_k-1} x_P\,(n;\boldsymbol{\tau}_{P-1})\,e^{-j2\pi fn}. \tag{3}$$

When the considered signal $x\,(n)$ is a monocomponent Pth order PPS, i.e.

$$x\,(n) = Ae^{j2\pi\sum_{m=0}^{P}\alpha_m(n\Delta)^m}, \tag{4}$$

where α_m are polynomial coefficients and Δ is the sampling interval, the Pth order ml-HIM of $x\,(n)$ is a complex sinusoid with frequency [14]

$$f = 2^{P-1}\Delta^P P!\alpha_P\prod_{k=1}^{P-1}\tau_k. \tag{5}$$

The coefficient α_P can be therefore estimated by searching for the position of maximum in the ml-HAF. Finding the position of maximum of the ml-HAF is usually performed in two stages, coarse search and fine search. The

coarse search represents finding the maximum bin of the ml-HAF. The fine search represents refining the coarse estimate through some iterative maximization method [18–20].

If we dechirp $x(n)$ by using the estimated value $\widehat{\alpha}_P$, i.e.

$$x'(n) = x(n)\, e^{-j2\pi\widehat{\alpha}_P (n\Delta)^P}, \tag{6}$$

the resulting signal $x'(n)$ will be the $(P-1)$th order PPS. Now the coefficient α_{P-1} can be estimated by searching for the position of maximum in the $(P-1)$th order ml-HIM of $x'(n)$. This procedure can be repeated to estimate all lower-order phase coefficients [12, Section III].

When the considered signal $x(n)$ is a multicomponent PPS, that is

$$x(n) = \sum_{k=1}^{K} A_k e^{j2\pi \sum_{m=0}^{P} \alpha_{k,m} (n\Delta)^m}, \tag{7}$$

where $\alpha_{k,m}$ are polynomial coefficients of the kth component, the Pth order ml-HIM will contain K sinusoids that correspond to autoterms, each having the frequency proportional to the highest order phase coefficient, according to (5). In addition to the autoterms, the ml-HIM will contain a large number of cross-terms which are, in general, Pth-order PPSs [14]. Specially, when the highest-order phase coefficients of some components coincide, the corresponding cross-terms are complex sinusoids, implying that some of the peaks in the ml-HAF correspond to the cross-terms [14]. Consequently, the maxima-based phase coefficients estimation is ambiguous, since a peak corresponding to a cross-term can lead to inaccurate estimation of the PPS's coefficients.

The effect of cross-terms can be significantly reduced using the PHAF proposed in [14]. In the PHAF, Q sets of time lags are used,

$$\mathbf{T}_{\mathbf{P-1}}^{\mathbf{Q}} = \left[\boldsymbol{\tau}_{\mathbf{P-1}}^{(\mathbf{1})}, \boldsymbol{\tau}_{\mathbf{P-1}}^{(\mathbf{2})}, \cdots, \boldsymbol{\tau}_{\mathbf{P-1}}^{(\mathbf{Q})}\right], \tag{8}$$

where $\boldsymbol{\tau}_{P-1}^{(l)} = \left[\tau_1^{(l)}, \tau_2^{(l)}, \cdots, \tau_{P-1}^{(l)}\right]$ and $l = 1, ..., Q$. The PHAF is defined as

$$X_P^Q(f, \mathbf{T}_{\mathbf{P-1}}^{\mathbf{Q}}) = \prod_{\mathbf{l=1}}^{\mathbf{Q}} \mathbf{X}_{\mathbf{P}}(\boldsymbol{\beta}^{(\mathbf{l})}\mathbf{f}, \boldsymbol{\tau}_{\mathbf{P-1}}^{(\mathbf{l})}), \tag{9}$$

with the scaling coefficient

$$\beta^{(l)} = \frac{\prod_{k=1}^{P-1} \tau_k^{(l)}}{\prod_{k=1}^{P-1} \tau_k^{(1)}}. \tag{10}$$

The PHAF uses the fact that the frequencies of autoterms in the ml-HIM are proportional to the product of used time lags. On the other hand, the frequencies of cross-terms are not proportional to this product. Therefore, the autoterms are enhanced more significantly in the PHAF than the cross-terms, since they are at the same positions in the scaled frequency for each ml-HAF, whereas the cross-terms are not aligned in the ml-HAFs obtained after the scaling over frequency.

How do we choose time lags? Authors in [14] suggest that the optimal lags for the Pth order ml-HAF are all equal to each other and to

$$\tau_{opt} = \frac{M}{2P}, \tag{11}$$

where M is the number of available samples. We will follow this suggestion.

C. Direct sequence spread-spectrum basics

In DS-SS systems, an SS signal to be transmitted, $s(n)$, is obtained by modulating each information bit by a pseudo-noise (PN) sequence $p(n)$ whose length is L chips. In addition, $p(n)$ is characterized by $E[p(n)] = 0$ and $E[p(n)\, p^*(m)] = \delta(n-m)$, where $E[\cdot]$ denotes the statistical expectation and $\delta(n)$ is the Dirac delta function [1]. The SS signal with 1 sample/chip will be assumed, when the perfectly flat spectrum is obtained [7].

At the receiver side, information bits are restored by correlating the baseband received signal $y(n)$ and a synchronized replica of the PN code, thus producing the decision variable

$$d = \sum_{n=0}^{L-1} y(n)\, p(n). \tag{12}$$

The measure of performance of the DS-SS receiver is the output signal-to-noise ratio (SNR_{out}) defined as [1, 2]

$$\mathrm{SNR}_{out} = \frac{E^2[d]}{\mathrm{Var}[d]}. \tag{13}$$

In particular, if $y(n)$ is composed of the SS signal and additive white Gaussian noise (AWGN) with zero mean and variance σ_w^2, the decision variable becomes

$$d = L + d_w, \tag{14}$$

where d_w is a Gaussian variable with zero mean and variance $L\sigma_w^2$. In this case,

$$\mathrm{SNR}_{out} = \frac{L}{\sigma_w^2}. \tag{15}$$

III. Jammer suppression

A. Statement of the problem

We will assume that the baseband received signal $y(n)$ contains three sequences as follows:

$$y(n) = s(n) + J(n) + w(n), \quad 0 \le n \le N-1, \tag{16}$$

where $s(n)$ is a unit amplitude SS signal, $J(n)$ is a complex-valued jammer and $w(n)$ is an AWGN sequence with zero mean and variance σ_w^2. The SNR is defined as $\mathrm{SNR} = 10\log_{10}\left(1/\sigma_w^2\right)$. All the three signals are uncorrelated with each other. We will also assume that $y(n)$ may contain several information bits, i.e., $L < N$.

The constant amplitude model for $J(n)$,

$$J(n) = Ae^{j\phi(n)}, \tag{17}$$

is used, where A and $\phi(n)$ respectively denote the amplitude of the jammer and its phase. Assuming that the original phase function $\phi(t)$ is continuous within the observed time interval, $\phi(n)$ can be approximated by a polynomial according to the Weierstrass's approximation theorem [9]. The signal-to-jammer ratio (SJR) is defined as $\mathrm{SJR} = 10\log_{10}\left(1/A^2\right)$.

For the received signal (16), the correlation (12) yields

$$d = L + d_J + d_w, \tag{18}$$

where d_J and d_w respectively represent the correlator outputs due to the jammer and AWGN. The central limit theorem (CLT) implies that, for large enough L, d_J can be well approximated by a white Gaussian variable with $E[d_J] = 0$ and $\mathrm{Var}[d_J] = LA^2$ [21]. The influence of a low power jammer is well mitigated by the correlation process, but when $J(n)$ is a high power jammer, $\mathrm{Var}[d_J]$ can dramatically reduce the SNR_{out}. In that case, $y(n)$ has to be preprocessed before the correlation is performed.

B. Monocomponent jammer suppression

We propose to divide the received signal into non-overlapping segments so that, for each segment separately, the jammer's phase $\phi(n)$ can be approximated by a third-order polynomial, or equivalently, the IF of the jammer can be approximated by a parabola. The estimated polynomial coefficients are used to dechirp the jammer, which is, in turn, suppressed by excising the corrupted low-pass frequency bins of the dechirped signal.

The jammer suppression can be performed in an adaptive manner by using the following recursive procedure.

***Step* 1.** Estimate the coefficients α_1, α_2 and α_3 of a polynomial that approximates the jammer's phase $\phi(n)$ by using the PHAF and the coefficient estimation procedure (see section II-B and (4)-(6)). We will denote the obtained estimations as $\widehat{\alpha}_1$, $\widehat{\alpha}_2$ and $\widehat{\alpha}_3$.

***Step* 2.** Form

$$\theta(n) = \widehat{\alpha}_1(n\Delta) + \widehat{\alpha}_2(n\Delta)^2 + \widehat{\alpha}_3(n\Delta)^3 \tag{19}$$

and dechirp $y(n)$ according to $y_\theta(n) = y(n)\,e^{-j2\pi\theta(n)}$.

***Step* 3.** Calculate $Y_\theta(k) = \mathrm{DFT}_k[y_\theta(n)]$. If the dechirped jammer occupies no more than K low-pass frequency bins, suppress it by setting corrupted bins to zero, which results in the filtered spectrum $Y_\theta^f(k)$. The filtered signal $y^f(n)$ is therefore obtained as

$$y^f(n) = \mathrm{IDFT}_n\left[Y_\theta^f(k)\right] e^{j2\pi\theta(n)}, \tag{20}$$

where $\mathrm{IDFT}_n[\cdot]$ represents the inverse discrete Fourier transform operator. On the other hand, if the dechirped jammer occupies more than K low-pass frequency bins, split the considered segment into two halves and perform the steps 1–3 for both halves separately. If,

however, the length of one half is less than the minimal considered length, do not split the segment but set all the corrupted frequency bins to zero and reconstruct the jammer-free segment according to (20).

In the first step of the algorithm, we essentially approximate the jammer's IF within the considered segment by a parabola determined by $\widehat{\alpha}_1$, $\widehat{\alpha}_2$ and $\widehat{\alpha}_3$. If it is well approximated within the whole signal of N samples, we suppress the jammer by excising the corrupted frequency bins of $y_\theta(n)$; otherwise, we split the signal into two halves and separately perform the IF estimation on both halves, first left then right. Reduced segment length implies reduced IF variation we deal with. If the IF estimation obtained for the left half (first N/2 samples) is sufficiently well, we filter the left half; otherwise, we split the left half into two halves and so on. Once we filter the current left half, we repeat the procedure for the corresponding right half. This way, the whole signal is adaptively split into non-overlapping segments and the length of each segment equals $N/2^p$, where $p = 0, 1, 2....$ Spectra of dechirped segments are illustrated in Fig.1, where we consider a jammer with sinusoidal phase, Type 5 in Table I. We first operate on N samples (Fig.1(a)), then on initial N/2 samples (Fig.1(b)) and finally on initial N/4 samples (Fig.1(c)). The first $N/4$ samples will not be further split since the jammer is well concentrated at the DC component, which is not the case for N and $N/2$.

We decide whether the jammer's IF is sufficiently well approximated by a parabola or not by comparing K low-pass frequency bins of $Y_\theta(k)$ to the predefined threshold Tr. In ideal case, when the parabola perfectly fits the jammer's IF, the whole jammer will be concentrated at $Y_\theta(0)$, implying $K = 1$ as a natural choice. In reality, however, estimated coefficients do not coincide with the true ones. In addition, the error-propagation effect makes the estimation of lower-order coefficients less accurate [12]. A non-polynomial phase inherently cannot be perfectly fit by a third-order polynomial. The dechirped jammer will be therefore spread over $Y_\theta(k)$ for $k \neq 0$; low-frequency components of $Y_\theta(k)$ will contain more jammer than the high-frequency ones (see Fig.1). Having this in mind, in this paper, we will say that the jammer's IF is sufficiently well approximated by a parabola if at most $K = 3$ low-pass frequency bins of $Y_\theta(k)$ (DC component and one bin from each side of the DC component) are corrupted.

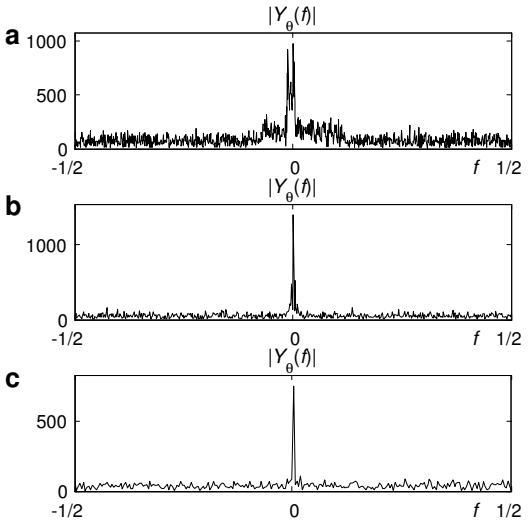

Fig. 1. The spectrum $|Y_\theta(f)|$ corrupted by a jammer with sinusoidal phase; f is normalized frequency. The parts correspond to first (a) N samples; (b) $N/2$ samples; (c) $N/4$ samples.

How to choose the threshold Tr? We will use the Neymann-Pearson criterion and choose Tr so that a fixed probability of false alarm (PFA) is provided. To this end, let us denote variable $Y_\theta(k)$ in the jammer-free case as Y_0. We can approximately model $|Y_0|$ as a Rayleigh variable. Indeed, in DS-SS systems, the AWGN can be much stronger than the SS signal [1] (see (15)), so their sum can be approximated by a Gaussian white noise with zero mean and variance that equals $\sigma_{sw}^2 = \sigma_s^2 + \sigma_w^2$, where σ_s^2 is the variance of the SS signal. Both real and imaginary part of Y_0 are therefore zero-mean Gaussian variables with common variance $\sigma_0^2 = \frac{N_1}{2}\sigma_{sw}^2$, where N_1 is the DFT length, implying that $|Y_0|$ is a Rayleigh variable with parameter $b = \sigma_0$. The mean

and variance of $|Y_0|$ satisfy [22]

$$\mu_{|Y_0|} = \sqrt{\frac{\pi}{2}}b \tag{21}$$

$$\sigma^2_{|Y_0|} = \left(2 - \frac{\pi}{2}\right)b^2. \tag{22}$$

We will herein take

$$Tr = \mu_{|Y_0|} + 4\sigma_{|Y_0|}, \tag{23}$$

which yields the PFA of $P(|Y_0| \geq Tr) = 5.5121 \times 10^{-4}$.

One way to estimate b, and, in turn, $\mu_{|Y_0|}$ and $\sigma_{|Y_0|}$, is to use TF representations of the received signal. For this purpose we will take the simplest TF representation, the STFT. In the TF plane, $J(n)$ occupies a narrow frequency band compared to both the SS signal and the AWGN that are spread over all frequencies. This allows for the estimation of $\mu_{|Y_0|}$ and $\sigma_{|Y_0|}$ from the STFT bins that belong to the TF areas where the jammer's contribution can be neglected.

What is the minimal segment length we consider? In order to reduce the computational complexity of the DFT calculation, we will take that the length of the signal block to be processed, N, satisfy $N = 2^m$, where m is a positive integer. After splitting, segments will be of the length $N_s = 2^{m-1}, 2^{m-2}...$ On each segment, we perform the coefficient estimation procedure based on the PHAF. Estimate $\widehat{\alpha}_3$ is obtained from the third-order ml-HIM of $y(n)$, $y_3(n;\boldsymbol{\tau}_2)$, whose length is $N_s - 2(\tau_1 + \tau_2)$ (see (2)). Taking (11) yields the length of $y_3(n;\boldsymbol{\tau}_2)$ of $N_s/3$, implying that small values of N_s cannot provide accurate estimate $\widehat{\alpha}_3$, which will emphasize the error-propagation effect. In this paper, we will adopt the minimal $N_s = 2^8 = 256$ samples, which gives the length of $y_3(n;\boldsymbol{\tau}_2)$ of 85 samples. We have experimentally shown that minimal $N_s = 128$ does not provide any gain over minimal $N_s = 256$, whereas $N_s < 128$ gives very poor accuracy to $\widehat{\alpha}_3$.

Finally, by observing the steps of the proposed method, as well as the computational complexity of the PHAF [14], we conclude that the overall computational complexity is $\mathrm{O}(N \log_2 N)$[1], where $\mathrm{O}(\cdot)$ represents the big O notation. On the other hand, the TF-based jammer suppression methods have the complexity of $\mathrm{O}\left(N^2 \log_2 N\right)$ [3,5].

C. Multicomponent jammer suppression

Taking into account the advantages of the PHAF regarding the estimation of multicomponent signals, the proposed algorithm can be easily extended to the multicomponent jammer case. Let us assume that the jammer contains N_J components that conform to model (17), i.e.

$$J(n) = \sum_{i=1}^{N_J} A_i e^{j\phi_i(n)}, \tag{24}$$

where A_i and $\phi_i(n)$ respectively denote the amplitude and phase of the ith component. Assuming that N_J is known [13, 14], we can suppress the jammer starting from the strongest component. The procedure is a modification of the estimation algorithm proposed in [13, Section II] and is given below.

***Step* 1.** Set $p = 1$.

***Step* 2.** If $p = N_J$ go to step 4. Otherwise, estimate the phase coefficients α_1, α_2 and α_3 of the strongest component and form $\theta(n)$ according to (19) (see steps 1 and 2 of the algorithm for the monocomponent jammer suppression).

***Step* 3.** Dechirp the received signal and suppress the strongest jammer component by setting at most K corrupted low-pass frequency bins to zero. Reconstruct the signal

[1]Consider the estimation of α_3 from an N samples long $y(n)$. It is estimated from the DFT of $y_3(n;\boldsymbol{\tau}_2)$. For $\tau_1 = \tau_2 = N/6$, $y_3(n;\boldsymbol{\tau}_2)$ has $N/3$ samples, and its calculation requires N complex multiplications (see (2)), or $4N$ real multiplications and $2N$ real additions, giving the complexity of $\mathrm{O}(N)$, for both multiplications and additions. On the other hand, the calculation complexity of an $N/3$ samples long DFT is $\mathrm{O}(N \log_2 N)$ multiplications and additions, which is also the complexity of the fine search frequency estimation [19]. The overall complexity of the α_3 calculation is therefore $\mathrm{O}(N \log_2 N)$. The similar reasoning holds for the α_2 and α_1 estimation. The dechirping operation in the algorithm requires N complex multiplications. The first two steps of the algorithm, therefore, require $\mathrm{O}(N \log_2 N)$ operations, and it can be easily seen that the same holds for the third step.

with the strongest component suppressed using (20). Set $p = p + 1$ and go to step 2.

***Step* 4.** Estimate $\theta(n)$ of the last component and dechirp the received signal. If the dechirped component occupies no more than K low-pass frequency bins, suppress it by setting corrupted bins to zero and reconstruct the jammer-free segment (20). Otherwise, perform the steps 1–3 for the left half and the right half of the observed signal. If the length of one half is less than the minimal considered length (256 samples), do not split the segment but set all the corrupted frequency bins to zero and reconstruct the jammer-free segment (20).

IV. Simulations

The performance of the proposed method is evaluated for the received signal corrupted by several jammer types. The phase functions of the considered jammers are given in Table I. The first three types correspond to a complex-sinusoid, linear FM (chirp) and quadratic FM jammer, respectively, whereas types 4 and 5 respectively conform to an exponential and sinusoidal model. In addition, $N = 1024$, $L = 64$, $\Delta = \frac{1}{N}$, SJR $= -25$dB and SNR $= -8$dB, i.e., $\sigma_w^2 = 6.31$. The analytical SNR_{out} value for the jammer-free received signal therefore equals 10.14 (see (15)). The third-order PHAF is calculated using five sets of time lags, given as follows: $\boldsymbol{\tau}_2^{(1)} = (\frac{N}{6}, \frac{N}{6}), \boldsymbol{\tau}_2^{(2)} = (\frac{11N}{75}, \frac{14N}{75}), \boldsymbol{\tau}_2^{(3)} = (\frac{17N}{120}, \frac{23N}{120}), \boldsymbol{\tau}_2^{(4)} = (\frac{19N}{150}, \frac{31N}{150}), \boldsymbol{\tau}_2^{(5)} = (\frac{7N}{60}, \frac{13N}{60})$, whereas the second-order PHAF is calculated using sets $\boldsymbol{\tau}_1^{(1)} = \frac{N}{4}, \boldsymbol{\tau}_1^{(2)} = \frac{N}{5}, \boldsymbol{\tau}_1^{(3)} = \frac{3N}{10}, \boldsymbol{\tau}_1^{(4)} = \frac{9N}{40}, \boldsymbol{\tau}_1^{(5)} = \frac{11N}{40}$. All time lags have to be rounded to the closest integer before use in the ml-HIM calculation. In time lags selection, we were guided by recommendation (11).

The proposed PHAF-based filtering is compared to the STFT-based filtering [3] and LPFT-based filtering [5,6]. Both in the STFT and LPFT calculation, the Hanning window with 128 samples is used. The obtained SNR_{out} and error probability (P_e) values for all the three methods are given in Table II. The first five rows of Table II correspond to the results obtained for monocomponent jammers defined in Table I. The sixth row represents results obtained in case of a multicomponent jammer that comprises the Type 2 and Type 3 components characterized by SJR $= -22$dB and -25dB, respectively. We also considered the case when the Type 3 jammer is passed through a multipath channel, resulting in a two-component jammer. The direct and delayed components are characterized by SJR $= -25$dB and -22dB, respectively. The delay is $N/7$. The obtained results are given in the last row of Table II; in Type 3_{d}, d stands for *delay*. For the monocomponent jammers, the proposed method slightly outperforms the other two methods. The difference in performance is more emphasized with multicomponent jammers, which is due to the fact that the proposed method is not affected by intersections of IF trajectories of jammer components. On the contrary, in the intersection area, the LPFT method cannot minimize the instantaneous bandwidth of jammer's components [5].

Figure 2. presents results obtained when variable SNR and SJR are considered. In specific, Fig. 2(a) and 2(b) present P_e and SNR_{out} curves versus SNR that varies from -15dB to -6dB, whereas Fig. 2(c) and 2(d) present P_e and SNR_{out} curves versus SJR that varies from -110dB to 0dB in increments of 5dB. In both cases, the Type 3 jammer is considered, and in the variable SNR case, it is characterized by fixed SJR $= -25$dB. In the variable SJR case, the AWGN with fixed SNR $= -8$dB is considered. The variable SNR case indicates that the proposed method slightly outperforms the other two methods for all the considered SNRs. On the other hand, in the variable SJR case, the difference in performance is much more emphasized for smaller SJRs. The LPFT and STFT curves depart from the PHAF one at around -40dB [5]. The proposed method performs approximately the same even for SJRs around -110dB. For SJR values close to 0, however, the parameter estimation in the proposed method does not produce accurate results, which results in performance degradation [18–20].

In this section, the numerical P_e and SNR_{out} values were calculated over 50000 runs, except

TABLE I
PHASE FUNCTIONS OF CONSIDERED JAMMERS

	Phase function $\phi(n)$
Type 1	$2\pi\frac{N}{5}(n\Delta)$
Type 2	$2\pi\left(-\frac{N}{3}(n\Delta)+\frac{N}{3}(n\Delta)^2\right)$
Type 3	$2\pi\left(\frac{N}{7}(n\Delta)-\frac{37N}{41}(n\Delta)^2+\frac{41N}{63}(n\Delta)^3\right)$
Type 4	$2\pi\left(\frac{2}{\ln\left(\frac{N}{2}\right)}\left(\frac{N}{2}\right)^{\frac{2}{3}}e^{\frac{\ln(N/2)}{3}(n\Delta)}-\frac{N}{4}(n\Delta)\right)$
Type 5	$2\pi\frac{N}{3\pi}\cos\left(\frac{7\pi}{9}(n\Delta)+\frac{\pi}{5}\right)$

TABLE II
P_e AND SNR_{out} VALUES FOR THE PHAF-, STFT- AND LPFT-BASED FILTERING

	SNR_{out}			P_e		
	PHAF	STFT	LPFT	PHAF	STFT	LPFT
Type 1	10.10	9.88	9.90	7.11e-4	8.37e-4	8.04e-4
Type 2	10.11	9.35	9.74	6.96e-4	1.11e-3	9.06e-4
Type 3	10.06	9.57	9.69	7.53e-4	1.04e-3	8.88e-4
Type 4	9.75	9.46	9.54	8.73e-4	9.69e-4	9.97e-4
Type 5	10.04	9.62	9.58	8.19e-4	1.05e-3	1.02e-3
Type 2 + Type 3	10.07	8.64	9.16	7.97e-4	1.76e-3	1.22e-3
Type 3 + Type 3_{d}	10.13	8.46	9.68	7.60e-4	2.01e-3	9.82e-4

for the curves in the variable SNR case which were simulated over 150000 runs.

V. Conclusion

In this paper, a simple and computationally efficient method for jammer suppression in DS-SS systems is proposed. The phase of the jammer is locally approximated by a polynomial, and its coefficients, estimated using the PHAF, are used to dechirp the received signal, thus dislocating the jammer to the low-pass frequency band. The jammer is successively suppressed by excising the corrupted frequency band of the received signal. In order to suppress jammers with non-polynomial phase, we developed an algorithm that adaptively divides the observed time interval so that, within each segment, the phase of the jammer can be satisfactorily approximated by a polynomial. The algorithm is extended so that it can suppress multicomponent jammers. Simulations show that the proposed method outperforms standard TF based methods used for jammer suppression, both in the error probability and calculation complexity.

References

[1] R. L. Pickholtz, D. L. Schilling, and L. B. Milstein, "Theory of spread-spectrum communications - a tutorial," *IEEE Transactions on Communications*, vol. 30, pp. 855-884, May 1982.

[2] M. G. Amin, "Interference mitigation in spread spectrum communication systems using time-frequency distributions," *IEEE Transactions on Signal Processing*, vol. 45, pp. 90-101, January 1997.

[3] X. Ouyang and M. G. Amin, "Short-time Fourier transform receiver for nonstationary interference excision in direct sequence spread spectrum communications," *IEEE Transactions on Signal Processing*, vol. 49, pp. 851-863, April 2001.

[4] O. Akay and G. F. Boudreaux-Bartels, "Broadband interference excision in spread spectrum communication systems via fractional Fourier transform," in *Conference Record of the Thirty-Second Asilomar Conference on Signals, Systems & Computers*, pp. 832-837, 1998.

[5] L. Stanković and S. Djukanović, "Order adaptive local polynomial FT based interference rejection in spread spectrum communication systems," IEEE Transactions on Instrumentation and Measurement, vol. 54, pp. 2156-2162, December 2005.

[6] S. Djukanović, M. Daković, and L. Stanković, "Local polynomial Fourier transform receiver for nonstationary interference excision in DSSS

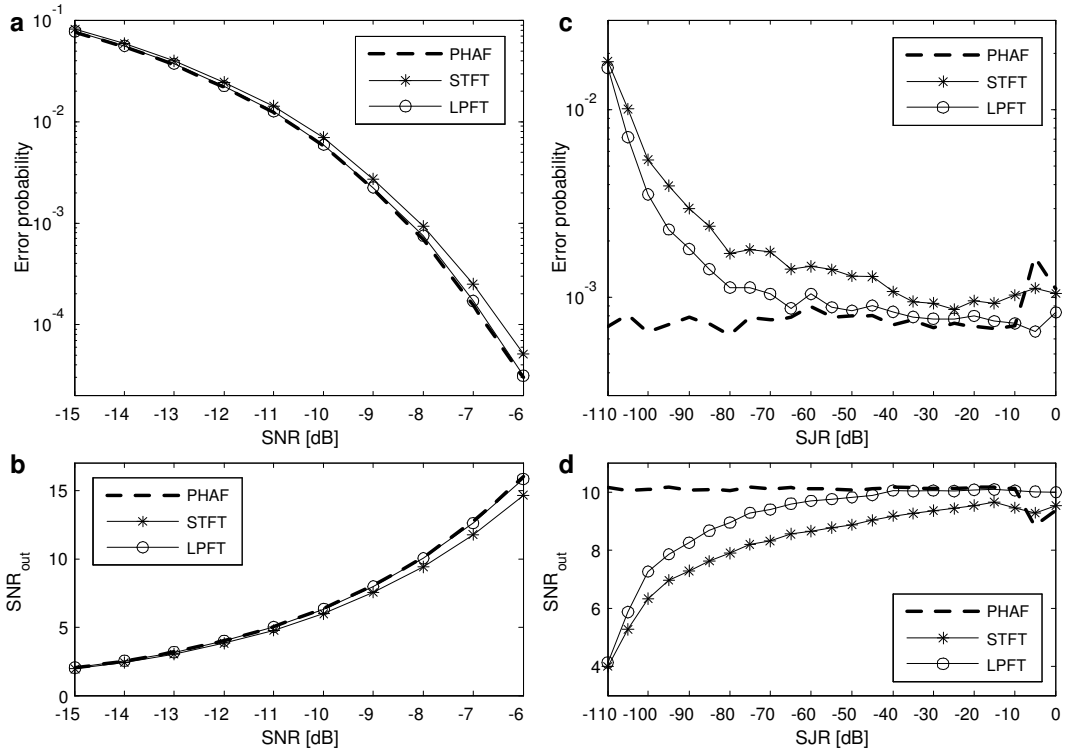

Fig. 2. (a) P_e versus SNR; SJR $= -25$dB. (b) SNR$_{out}$ versus SNR; SJR $= -25$dB. (c) P_e versus SJR; SNR $= -8$dB. (d) SNR$_{out}$ versus SJR; SNR $= -8$dB. In all the cases, the Type 3 jammer is considered.

communications," *IEEE Transactions on Signal Processing*, vol. 56, pp. 1627-1636, April 2008.

[7] J. A. Young and J. S. Lehnert, "Analysis of DFT-based frequency excision algorithms for direct-sequence spread-spectrum communications," *IEEE Transactions on Communications*, vol. 46, pp. 1076-1087, August 1998.

[8] B. Boashash, *Time-frequency signal analysis and processing*. Elsevier Science, 2003.

[9] A. Papoulis, P*robability, random variables, and stochastic processes*. McGraw-Hill Companies; 3rd edition, 1991.

[10] S. Peleg and B. Porat, "Estimation and classification of polynomial phase signals," *IEEE Transactions on Information Theory*, vol. 37, pp. 422-430, March 1991.

[11] B. Boashash, "Estimating and interpreting the instantaneous frequency of a signal - part 2: Algorithms and applications," *Proceedings of the IEEE*, vol. 80, pp. 540-568, April 1992.

[12] S. Peleg and B. Friedlander, "The discrete polynomial-phase transform," *IEEE Transactions on Signal Processing*, vol. 43, pp. 1901-1914, August 1995.

[13] S. Peleg and B. Friedlander, "Multicomponent signal analysis using the polynomial-phase transform," *IEEE Transactions on Aerospace and Electronic Systems*, vol. 32, pp. 378-387, January 1996.

[14] S. Barbarossa, A. Scaglione, and G. B. Giannakis, "Product high-order ambiguity function for multicomponent polynomial phase signal modeling," *IEEE Transactions on Signal Processing*, vol. 46, pp. 691-708, March 1998.

[15] D. Pham and A. M. Zoubir, "Analysis of multicomponent polynomial phase signals," *IEEE Transactions on Signal Processing*, vol. 55, pp. 56-65, January 2007.

[16] V. Popović, I. Djurović, L. Stanković, T. Thayaparan, and M. Daković, "Autofocusing of SAR images based on parameters estimated from the PHAF," *Signal Processing*, vol. 90, pp. 1335-1754, May 2010.

[17] V. Katkovnik, "A new form of the Fourier transform for time-varying frequency estimation," *Signal Processing*, vol. 47, pp. 187-200, November 1995.

[18] Y. V. Zakharov and T. C. Tozer, "Frequency estimator with dichotomous search of periodogram peak," *Electronics Letters*, vol. 35, pp. 1608-1609, September 1999.

[19] Y. V. Zakharov, V. M. Baronkin, and T. C. Tozer, "DFT-based frequency estimators with narrow acquisition range," *IEE Proceedings Communications*, vol. 148, pp. 1-7, February 2001.

[20] E. Aboutanios and B. Mulgrew, "Iterative frequency estimation by interpolation on Fourier coefficients," *IEEE Transactions on Signal Process-*

ing, vol. 53, pp. 1237-1242, April 2005.

[21] S. Djukanović, M. Daković, and L. Stanković, "Bit error probability approximation for short-time Fourier transform based nonstationary interference excision in DS-SS systems," *Signal Processing*, vol. 89, pp. 2178-2184, November 2009.

[22] A. Papoulis and U. S. Pillai, *Probability, random variables, and stochastic processes*. McGraw Hill Higher Education; 4th edition, 2002.